

Time-Varying Causal Treatment for Quantifying the Causal Effect of Short-Term Variations on Arctic Sea Ice Dynamics

Akila Sampath¹, Vandana P. Janeja¹, and Jianwu Wang¹

¹ 1 Department of Information Systems, University of Maryland, Baltimore County, Baltimore, MD, United States

² Institute for Harnessing Data and Model Revolution in the Polar Regions (iHARP)
`{asampath,vjaneja,jwang}@umbc.edu`

Abstract. Quantifying the causal relationship between ice melt and freshwater distribution is critical, as these complex interactions manifest as regional fluctuations in sea surface height (SSH). Leveraging SSH as a proxy for sea ice dynamics enables improved understanding of the feedback mechanisms driving polar climate change and global sea-level rise. However, conventional deep learning models often struggle with reliable treatment effect estimation in spatiotemporal settings due to unobserved confounders and the absence of physical constraints. To address these challenges, we propose the Knowledge-Guided Causal Model Variational Autoencoder (KGCM-VAE) to quantify causal mechanisms between sea ice thickness and SSH. The proposed framework integrates a velocity modulation scheme in which smoothed velocity signals are dynamically amplified via a sigmoid function governed by SSH transitions to generate physically grounded causal treatments. In addition, the model incorporates Maximum Mean Discrepancy (MMD) to balance treated and control covariate distributions in the latent space, along with a causal adjacency-constrained decoder to ensure alignment with established physical structures. Experimental results on both synthetic and real-world Arctic datasets demonstrate that KGCM-VAE achieves superior PEHE compared to state-of-the-art benchmarks. Ablation studies further confirm the effectiveness of the approach, showing that the joint application of MMD and causal adjacency constraints yields a 1.88% reduction in estimation error.

Keywords: Causal Inference, Sea Ice Thickness, Time-varying treatment, Causal Mechanism, Knowledge Guidance

1 Introduction

Earth system data exhibit large variability, stemming from climate model simulations and real-world observational data, leading to the increased use of machine learning (ML) and statistical methods to find patterns in the respective systems [1]. However, despite their strong predictive ability, current ML and deep learning methods have limitations in understanding the underlying cause-and-effect

relationships between variables [1, 2], which is crucial for process understanding. Causal inference combines domain knowledge, machine learning models, and observational or interventional data [3, 2] to identify a system’s underlying causal structure and quantify its effects.

In this study, our objective is to move beyond correlation and estimate the total causal effect of sea surface height (SSH) on sea ice thickness. This chosen real-world scenario represents a highly impactful contribution because the two phenomena are critically linked to global climate change. Changes in SSH are a key factor in monitoring sea level rise, and the complex, non-direct influence of SSH dynamics on sea ice thickness through mechanisms like ocean circulation and freshwater distribution is a significant, yet difficult-to-quantify, area of climate research. Quantifying this non-direct causal effect is crucial for refining climate models and enhancing predictability. For this purpose, we propose a novel, specialized VAE-based architecture: the Knowledge-Guided Causal Modeling Variational Autoencoder (KGCM-VAE). This unique framework is designed to leverage the flexibility of VAEs and causal modeling to provide robust estimates of the total causal effect in such complex, indirect systems.

To address this complexity, we first rely on a qualitative literature review [4–6] to inform the construction of a preliminary causal (time series) graph. This graph helps identify observed and unobserved confounding variables and potential connections between Arctic climate drivers and sea ice thickness. While Arctic climate drivers are known to influence sea ice thickness, our causal effect estimation is designed to quantify this influence precisely, especially when considering a graph of other observed and unobserved variables.

Deeper understanding of a system requires combining causal inference with predictive machine learning, as it reveals insights that go beyond mere correlations [7]. Traditional predictive machine learning has demonstrated remarkable success in discerning patterns and generating predictions from data. However, these models primarily uncover correlations, often lacking a deep, theoretical understanding of the system’s true causal mechanisms. Judea Pearl argues that incorporating causal understanding into machine learning is essential for advancing beyond correlation-based predictions, empowering models to perform more reliably in new settings, improving their ability to handle unseen scenarios and cross-domain shifts [2].

Answering fundamental causal questions depends on accurately modeling how a treatment variable influences an outcome’s distribution [8, 9]. However, inferring these relationships from observational data is highly challenging, primarily due to unmeasured confounders [10, 11]. These hidden factors simultaneously affect both the observed treatment and the outcome, creating spurious correlations that obscure true causal pathways. Challenges such as fairness, generalization to unseen data, and domain adaptation often stem from these underlying causal complexities, which causal inference [10, 11] aims to mitigate by learning robust data representations that facilitate the estimation of true causal effects.

Climate research often relies on simulated models to discover causal dynamics, but trust in these outcomes is determined by the realism of the simulated physics compared to reality. Consequently, there's a critical demand for deriving causal connections directly from real-world time series [12, 1, 13], enabling data-driven insights that are grounded in observed phenomena rather than solely in model-based assumptions. Therefore, we aim to address a pivotal problem in both AI and causality by identifying abstract causal variables from concrete, low-level observations [14]. The main contributions in this paper are as follows:

1. We present the KGCM-VAE, a novel architecture that successfully integrates Maximum Mean Discrepancy (MMD)-based latent deconfounding within a recurrent VAE framework specifically designed for causal modeling.
2. Our method discovers the underlying structural dependencies (the adjacency matrix) among the variables directly from the data, providing a scientific advantage over models that require pre-defined or fixed relationships.
3. We demonstrate our KGCM-VAE provides highly reliable, unbiased estimates of time-varying causal effects, moving beyond correlation to accurately quantify treatment impact in complex sequential systems.

2 Related Work

Causal inference approaches are typically divided into parametric and non-parametric methods, depending on the assumptions made about the structure of the relationships among variables [15]. In non-parametric approaches such as nearest-neighbor matching, propensity score matching, and propensity score re-weighting, the context-intervention-outcome relationship is not modeled explicitly [15]. Parametric methods such as linear and logistic regression, as well as structured models like random forests and regression trees, build explicit mappings to model the relationship between covariates, treatment, and outcomes [16, 17]. Doubly robust approaches combine models for both the outcome and the treatment assignment, allowing for consistent estimation even if only one of the models is correctly specified [18]. However, these methods are efficient only when the treatment assignment probability is known. Machine learning methods like tree based methods are increasingly being adapted for causal effect inference, notably for individual-level treatment effects [17, 19]. In addition to tree-based models, researchers have shown that high dimensional regression techniques like Lasso can be adapted to reliably estimate treatment effects, attaining convergence rates comparable to those in semi-parametric settings [20, 19]. Representation learning offers a compelling approach to counterfactual inference by learning embeddings that help address the challenge of unobserved potential outcomes [27, 22]. Although the SITE (Similarity-Preserved Individual Treatment Effect) framework leverages deep representation learning for estimating individual treatment effects, it generally lacks mechanisms to capture intricate time lagged temporal relationships [23]. Moreover, current studies often struggle to preserve or utilize the essential "similarity information" that is

structured across space and time, or that manifests through complex, non-linear interactions within the underlying physical system. While [24] demonstrated that balance can be achieved through strategic covariate selection and by modeling the interactions between treatments and covariates, many existing frameworks fail to effectively incorporate the temporal dynamics inherent in time-varying treatments. Furthermore, standard neural networks lack the inherent physical grounding required to distinguish between spurious correlations and true causal relationships.

To address these limitations, our proposed method incorporates knowledge-guided treatment effect generation to accurately account for real-world, time-varying information. Specifically, our methodology introduces knowledge guidance derived from established physical phenomena. Complementing this, our approach adopts a causal adjacency mechanism [29, 30] that enables the neural network to automatically detect and enforce the underlying causal connections between features. This dual-strategy ensures that the model is structurally constrained by physical laws while remaining flexible enough to learn complex dependencies from data.

3 Data and Problem Formulation

3.1 Data

The primary data source for this research is the Subseasonal to Seasonal (S2S) ECMWF Real-time Control Forecast. This dataset serves as a critical bridge between short-term atmospheric modeling and long-term climate projections. The study focuses on a temporal span of 1,620 days, covering the period from January 2020 through June 2024. To isolate the physical dynamics of the Arctic environment, the global 1° grid (360×181) was subsetted to the high northern latitudes, specifically the region between 60°N and 90°N . To address the computational complexity and focus on regional-scale physical trends, a spatial averaging preprocessing step was implemented. This involved computing daily time series by averaging each physical parameter—specifically sea-ice thickness, sea surface height, and tri-component seawater velocities (eastward, northward, and total)—across the spatial grid. This transformation converts the high-dimensional spatial data into a robust, multivariate daily time series suitable for PhysE-Inv analysis.

3.2 Problem Formulation

The primary objective of this study is to quantify the causal effect of short-term oceanic drivers, denoted as treatment T , on Arctic sea ice thickness, denoted as the outcome Y , by leveraging a knowledge-guided causal modeling framework that accounts for historical temporal dependencies. Given a historical lookback window (lag) of length L , we define the input space at time step t and location i using a sequence of historical covariates $\mathbf{X}_{t-L+1:t,i}$ and historical treatments

$\mathbf{T}_{t-L+1:t,i}$. The covariates consist of feature variables derived from oceanic conditions, such as velocities and raw sea surface height, observed over the past L time steps. We distinguish between two treatment sequences: the factual (observed) unmodulated signal sequence T_1 , and the counterfactual (intervened) velocity-modulated signal sequence T_2 .

To capture the temporal dynamics, the potential outcomes are defined as a function of the historical trajectories of both covariates and treatments:

$$Y_{t+n,i}(T_j) = f(\mathbf{X}_{t-L+1:t,i}, \mathbf{T}_{j,t-L+1:t,i}) \quad (1)$$

where $Y_{t+n,i}$ represents the predicted sea ice thickness at a future lead time n . The central goal is to estimate the Individual Treatment Effect (ITE) across the temporal lag, defined as:

$$\tau = Y_{t+n,i}(T_1) - Y_{t+n,i}(T_2) \quad (2)$$

This formulation allows the model to isolate the specific causal influence of oceanic shifts by comparing the factual historical sequence against a physically-informed counterfactual intervention.

4 Methodology

4.1 Knowledge Guidance

The KGCM-VAE framework incorporates domain-specific physical constraints to guide the learning of causal relationships within the Arctic system. A primary pillar of this guidance is the established hydrostatic relationship between SSH and sea ice thickness, which is essential for confirming the reliability of causal estimates in ice-covered oceans. The physical interaction is governed by the following equilibrium equation:

$$h_i = (h_{\text{ice}} - h_{\text{ssh}}) \left(\frac{\rho_w}{\rho_w - \rho_i} \right) - h_s \left(\frac{\rho_w - \rho_s}{\rho_w - \rho_i} \right)$$

where h_i denotes the sea ice thickness, h_{ice} represents the total freeboard (ice plus snow), h_{ssh} is the sea surface height, and h_s denotes snow depth. The parameters ρ_w , ρ_i , and ρ_s correspond to the densities of seawater, sea ice, and snow, respectively. By embedding the knowledge from this relationship, the model ensures that the predicted treatment effects of SSH on ice thickness remain physically consistent. Furthermore, the framework utilizes the connection between SSH and surface velocity to capture the underlying Arctic ocean dynamics. This relationship is defined through geostrophic balance, where the surface velocity components (u, v) are determined by the spatial gradients of the SSH:

$$u = -\frac{g}{f} \frac{\partial \eta}{\partial y}, \quad v = \frac{g}{f} \frac{\partial \eta}{\partial x}$$

Here, g represents the acceleration due to gravity, f is the Coriolis parameter, and the terms $\frac{\partial \eta}{\partial x}$ and $\frac{\partial \eta}{\partial y}$ represent the spatial slopes of the SSH. Integrating knowledge of these geostrophic equations in treatment generation allows the model to differentiate between thermodynamic changes and those driven by ocean-ice dynamics, such as ice drift and surface gradient forces.

4.2 Knowledge-Guided treatment generation

In time-series causal inference, the primary challenge is confounding. We aim to determine if a change in the lagged treatment ($T_{t-\text{lag}}$, modulated SSH) truly *causes* a change in the future outcome (Y , ice thickness). A reliable causal estimate requires that samples receiving different treatments are comparable based on their baseline characteristics. We utilize a novel SSH-velocity modulation scheme to create a physically-guided treatment signal. This scheme addresses the challenges of time-varying treatment effect in quantifying the causal effect. To capture sub-seasonal variability, a moving window filter formulation is applied, resulting in the smoothed SSH signal. The smoothed sea surface height ($\overline{\text{SSH}}_t$) signal is dynamically amplified via a sigmoid function controlled by the total velocity. Our treatment scheme thus generates a robust, physically-guided signal (x_t^{treat}) that enhances the model's ability to quantify the effect on sea ice thickness. The overall amplification is controlled by the modulation factor σ_t , computed using the following sigmoid function:

$$\sigma_t = \frac{1}{1 + \exp[-a(\tilde{v}_t - v_0)]} \quad (3)$$

In this equation, \tilde{v}_t is the smoothed total velocity, v_0 is the transition center (controlling the velocity threshold for amplification), and a is the steepness parameter (controlling the sigmoid's curve).

The smoothed SSH signal ($\overline{\text{SSH}}_t$) is then modulated by the factor $(1 + \beta\sigma_t)$, where β is the overall modulation strength parameter. The final velocity-modulated SSH signal ($\text{SSH}_t^{\text{treat}}$) is calculated by the formula:

$$\text{SSH}_t^{\text{treat}} = (1 + \beta\sigma_t)\overline{\text{SSH}}_t \quad (4)$$

This treated signal $\text{SSH}_t^{\text{treat}}$ is subsequently used as a covariate in the downstream prediction model.

4.3 Synthetic data generation

We generate synthetic counterfactual outcome data to evaluate the causal inference capabilities of the proposed model under controlled conditions. The data generation process is designed to reflect a known non-linear physical relationship between treatment and outcome, enabling a direct assessment of whether the model can recover the imposed causal structure.

Specifically, the synthetic counterfactual outcome is defined as

$$\mathbf{Y}_{1,t} = \mathbf{Y}_{0,t} + \beta \cdot \tanh(\alpha \cdot (\mathbf{T}_{1,t} - \mathbf{T}_{0,t} - \mu_{\mathbf{T}})) + \epsilon, \quad (5)$$

where $\mathbf{Y}_{0,t}$ denotes the observed factual outcome and $\mathbf{T}_{1,t}$ and $\mathbf{T}_{0,t}$ represent the treated and factual treatment variables, respectively. The treatment difference is centered by the mean treatment difference $\mu_{\mathbf{T}}$, ensuring stability across samples. The hyperbolic tangent function introduces a bounded and non-linear causal effect, while the parameters α and β control the steepness and magnitude of this effect. An additive noise term ϵ is included to capture realistic variability.

This formulation isolates the direct causal influence of the treatment on the outcome by excluding explicit confounding variables, allowing for a focused evaluation of the model's ability to learn non-linear causal relationships. By grounding the synthetic data in known physical principles, this approach provides a reliable and interpretable benchmark for validating causal effect estimation in time series settings.

4.4 Model Architecture

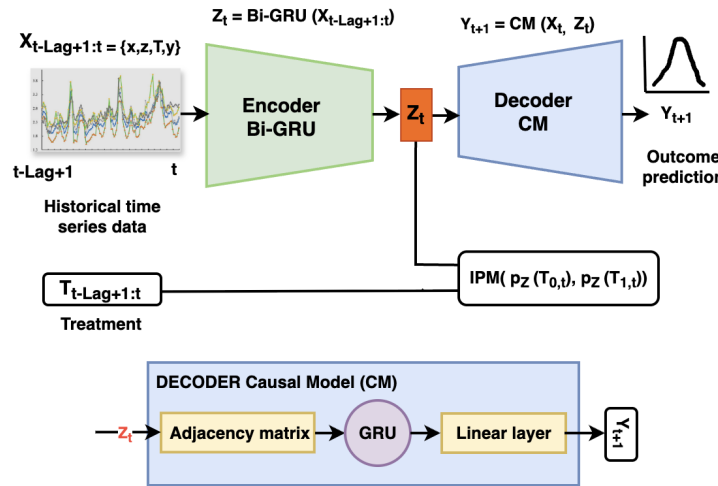


Fig. 1. The Architecture of the Knowledge-Guided Causal Model Variational Autoencoder (KGCM-VAE) integrates a balanced latent space \mathbf{z} learned by the encoder with a knowledge-guided causal model in the decoder for robust counterfactual prediction and Individual Treatment Effect estimation.

Knowledge-Guided Causal Modeling (KGCM-VAE) Framework: The KGCM-VAE framework (Figure 1) is an architecture designed to estimate time-varying causal effects by addressing temporal confounding and enabling structural discovery within sequential data. The model extends the standard variational autoencoder framework by incorporating specific structural constraints

and regularization components to ensure robust causal inference. The system is composed of two primary modules: a recurrent encoder that extracts temporal features and a causal decoder that performs structural interventions. We denote the input time series as $\mathbf{X} \in \mathbf{R}^{T \times p}$, the latent representation as \mathbf{Z}_t , and the learned adjacency mask as \mathbf{M} .

Encoder and Latent Representation: To capture the unobserved factors governing the joint dynamics of the Arctic system, the framework employs a Bidirectional Gated Recurrent Unit (Bi-GRU). Let $\mathbf{X} \in \mathbf{R}^{B \times T \times p}$ denote a batch of multivariate time series comprising physical covariates, treatment variables, and lagged treatments. The encoder processes a fixed look-back window, $\mathbf{X}_{t-Lag+1:t}$, and maps it to a latent vector $\mathbf{Z}_t \in \mathbf{R}^{d_z}$:

$$\mathbf{Z}_t = \text{Bi-GRU}(\mathbf{X}_{t-Lag+1:t}) \quad (6)$$

The latent dimension is fixed to $d_z = 32$, providing a compact yet expressive representation of historical context while maintaining computational efficiency. This representation captures the background environmental state required for unbiased counterfactual estimation.

Causal Decoder (CM): The decoder is implemented as a Causal Model (CM) that explicitly incorporates the structural arrangement of physical influences within the climate system. The model uses the connection matrix to gate the influence of treatments, ensuring that predictions are governed by hypothesized causal pathways. The decoder reconstructs the outcome based on the latent state \mathbf{Z}_t and an adjacency mask $\mathbf{M} \in \mathbf{R}^{p \times p}$ derived from learnable logits and prior knowledge. To enforce these causal constraints, the input to the i -th GRU unit, Input_i , is defined as the concatenation of the latent state \mathbf{Z}_t and the masked features from the previous time step \mathbf{X}_{t-1} :

$$\text{Input}_i = [(\mathbf{X}_{t-1} \odot \mathbf{M}_{i,\cdot}), \mathbf{Z}_t]$$

In this formulation, $M_{i,j}$ acts as a binary gate: if $M_{i,j} = 1$, the j -th feature from \mathbf{X}_{t-1} is passed to the i -th unit; if $M_{i,j} = 0$, the feature is blocked. This mechanism ensures that information propagation strictly follows the learned or predefined causal structure of the Arctic system.

Causal Connection Matrix for Temporal Dependency: In this study, we include both the instantaneous treatment T_t and its lagged counterpart $T_{t-\text{lag}}$ to reflect that climate systems exhibit both immediate forcing and delayed physical responses. Excluding T_t would prevent the model from capturing contemporaneous effects, potentially forcing lagged variables to explain variability they do not causally generate. Such omissions lead to causal misidentification, where $T_{t-\text{lag}}$ acts as a proxy for T_t , resulting in biased causal attribution and misleading PEHE estimates. To model these dependencies, the adjacency mask \mathbf{M} serves as a hard architectural constraint on information flow. Unlike standard neural networks that assume dense, unconstrained connectivity, this matrix explicitly

encodes permitted causal paths. Entries with $M_{ij} > 0$ define active paths, while zero entries strictly prohibit influence by masking the corresponding network weights. In the absence of prior knowledge, an identity matrix would isolate each variable; instead, we deliberately enable causal edges from both T_t and T_{t-lag} to the outcome variable Y . This design ensures the model represents realistic ocean–ice interactions governed by physical time lags while remaining structurally blind to spurious feedback loops. This controlled information flow is critical for counterfactual inference, ensuring that the estimated PEHE reflects true temporal causality rather than artifacts of unrestricted connectivity.

Temporal Discretization and Delayed Treatment Effects: To structure the temporal data for causal analysis, we implement a sliding window formulation with a look-back parameter L . At each time step t , the input features $(\mathbf{X}_t, \mathbf{T}_t)$ span a fixed window $[t - L + 1, t]$ that captures the historical context required for the Bi-GRU encoder. The target outcome Y_{t+n} is situated at a future lead time n , ensuring that future states are predicted solely from historical information, thereby enforcing a valid temporal structure for causal inference. Recognizing that climate systems exhibit delayed responses, we account for lagged effects by shifting the treatment signal: $\mathbf{T}_{lag}(t) = \mathbf{T}(t - 1)$. This design choice encodes the physical assumption that oceanic interventions propagate through the system before influencing sea ice thickness. During training, the framework is optimized using two potential outcome trajectories—factual and counterfactual—in parallel. Specifically, the model is conditioned on the same covariate history but trained on $(\mathbf{X}, \mathbf{T}_{lag}^{(1)}, \mathbf{Y}^{(1)})$ and $(\mathbf{X}, \mathbf{T}_{lag}^{(2)}, \mathbf{Y}^{(2)})$ simultaneously. This dual-trajectory optimization enables the model to perform robust counterfactual estimation while maintaining strict adherence to temporal causality.

Integral Probability Metric (IPM): In time-series causal inference, the primary challenge is confounding. We aim to determine if a change in the lagged treatment (T_{t-lag} , modulated SSH) truly causes a change in the future outcome (Y , sea ice thickness).

To address confounding bias, we introduce a statistical constraint in the latent space (Z) that compels the model to achieve causal balance (covariate balance). The constraint requires matching the distribution of latent factors between the treated and control samples.

$$P(Z | T = 1) \approx P(Z | T = 0)$$

The Maximum Mean Discrepancy (MMD): This metric provides a robust and differentiable measure of the difference between these two distributions, $P = P(Z | T = 0)$ and $Q = P(Z | T = 1)$. By minimizing the IPM value, we train the encoder to produce balanced latent representations Z .

We utilize MMD, a kernel-based IPM, to rigorously quantify the distance between the treated and control latent distributions. This statistical measure is defined as:

$$MMD^2(P, Q) = E_{x, x' \sim P}[k(x, x')] + E_{y, y' \sim Q}[k(y, y')] - 2E_{x \sim P, y \sim Q}[k(x, y)]$$

Here, $k(\cdot, \cdot)$ is a positive-definite kernel function (such as an RBF kernel), and $E[\cdot]$ denotes the expectation.

The core of this mechanism is the radial basis function (RBF) kernel (or Gaussian kernel), which measures the similarity between every pair of latent vectors by implicitly mapping them into a high-dimensional feature space. The RBF kernel is defined as:

$$k(x, y) = \exp\left(-\frac{\|x - y\|^2}{2\sigma^2}\right)$$

In this function, $\|x - y\|^2$ is the squared Euclidean distance between two vectors. The parameter σ controls the width of the kernel; smaller σ makes the kernel more sensitive to small differences.

The final MMD value is calculated as an empirical estimate of the squared distance (MMD^2). This calculation involves three key terms: The first term, $E_{x, x' \sim P}[k(x, x')]$, measures similarity within the treated distribution. The second term, $E_{y, y' \sim Q}[k(y, y')]$, measures similarity within the control distribution (Control Self-Similarity). The third term, $-2E_{x \sim P, y \sim Q}[k(x, y)]$, measures similarity between the treated and control distributions. A smaller MMD value indicates that the distributions are more similar. Specifically, an MMD score of zero indicates that the latent distributions $P(Z | T = 1)$ and $P(Z | T = 0)$ are statistically indistinguishable, confirming successful causal balance.

This MMD term is incorporated into the VAE's total loss function. Minimizing it ensures the encoder learns representations \mathbf{z} where covariate distributions for treated and control groups are brought into close proximity. This effectively makes the conditional ignorability assumption more robust with respect to observed covariates in the representation space. The resulting MMD value also serves as a quantifiable measure of covariate balance achieved.

MSE Loss: This component quantifies the discrepancy between the model's predicted outcome \hat{Y} and the observed true outcome Y . It drives the model towards high predictive accuracy. The equation for the MSE loss is:

$$\mathcal{L}_{\text{pred}} = \frac{1}{N} \sum_{i=1}^N (\hat{Y}_i - Y_i)^2$$

KL Divergence Loss: This regularization term, inherent to Variational Autoencoder (VAE) architectures, encourages the learned latent distribution (parameterized by its mean μ and log-variance $\log \sigma^2$) to conform to a standard normal distribution. This component ensures the development of a well-structured, generalizable, and disentangled latent representation. The equation for the KL Divergence loss is:

$$\mathcal{L}_{\text{KL}} = -0.5 \sum_{j=1}^D (1 + \log \sigma_j^2 - \mu_j^2 - e^{\log \sigma_j^2})$$

where D is the dimensionality of the latent space.

Total Loss: The KGCM-VAE is trained by minimizing a unified loss function $\mathcal{L}_{\text{total}}$, balancing reconstruction fidelity, latent regularization, deconfounding, and structural sparsity:

$$\mathcal{L}_{\text{Total}} = \mathcal{L}_{\text{pred}} + \alpha \mathcal{L}_{\text{KL}} + \beta \mathcal{L}_{\text{MMD}}$$

The total loss is a weighted sum of three terms: $\mathcal{L}_{\text{Reconstruction}}$, which measures reconstruction fidelity by ensuring predicted outcomes (\hat{Y}) match ground truth (Y); \mathcal{L}_{KL} , which enforces structure in the latent space by minimizing the Kullback-Leibler (KL) divergence between the latent distribution $P(Z)$ and a standard Gaussian prior $\mathcal{N}(0, I)$; and \mathcal{L}_{MMD} , which enforces the Causal Balance constraint by minimizing the Maximum Mean Discrepancy to ensure treatment independence in the latent space Z .

4.5 Evaluation Metrics

We assess the causal inference performance of the KGCM-Decoder by estimating the Individual Treatment Effect (ITE) at a specific lag ℓ , which quantifies the temporal impact of oceanic drivers. The ITE for a specific sample at time t with a prediction horizon ℓ is defined as the difference between the potential outcomes under the treated ($A_t = 1$) and control ($A_t = 0$) conditions, conditioned on the historical covariate sequence $X_{0:t}$:

$$\tau(t, \ell) = Y^{(1)}(t + \ell \mid A_t = 1, X_{0:t}) - Y^{(0)}(t + \ell \mid A_t = 0, X_{0:t}) \quad (7)$$

where $t + \ell$ represents the future time step at which the sea ice thickness outcome is measured. To evaluate the model's accuracy in capturing these heterogeneous causal effects, we employ the Precision in Estimation of Heterogeneous Effects ($PEHE_{\text{lag}}$) metric. This metric calculates the mean squared error between the estimated ITE ($\hat{\tau}$) and the ground-truth ITE (τ) derived from physical simulations across all N temporal samples:

$$PEHE_{\text{lag}} = \frac{1}{N} \sum_{i=1}^N (\hat{\tau}_i(t, \ell) - \tau_i(t, \ell))^2 \quad (8)$$

By utilizing this lagged formulation, the model specifically penalizes errors in the predicted response of sea ice to treatment interventions based on the accumulated historical context.

4.6 Baselines

To evaluate the performance of our proposed KGCM-VAE, we benchmark it against three prominent deep learning architectures tailored for time-series causal inference. A common feature of these comparison methods is their capacity to predict unobserved counterfactual outcomes, enabling the estimation of the Individual Treatment Effect (ITE).

1. **Counterfactual Recurrent Neural Network (CF-RNN)** [25]: This model is specifically designed for sequential causal inference. It operates by learning disentangled representations to explicitly model both factual and counterfactual time-series sequences. It achieves this by ensuring that the representation is predictive of the outcome while remaining invariant to treatment assignment.
2. **Causal Recurrent Neural Network (Causal RNN)** [26]: This refers to a general recurrent neural network architecture adapted for time-series causal inference. The model is typically trained using techniques (such as an adversarial loss or a MMD penalty) to learn temporal representations that aim to control for confounding variables over time, thereby satisfying the sequential unconfoundedness assumption.
3. **Causal TaRNET** [27]: TaRNET is a foundational deep learning architecture for causal inference. While originally designed for static data, we adapt its two separate prediction heads for the treated and control groups into a recurrent architecture for time-series data (Causal TaRNET). This structure is designed to learn balanced latent representations by sharing a common embedding layer and utilizing distinct prediction heads to facilitate robust counterfactual prediction and ITE estimation.

While these baseline models were originally developed for different use cases, we carefully modify their architectures and training procedures (e.g., integrating similar recurrent units and sequence-to-sequence structures) to ensure an effective and fair comparison with our proposed KGCM-VAE approach.

The code and modified implementations for all baselines are made publicly available for reproducibility. The GitHub repository link can be found at <https://anonymous.4open.science/KGCM-VAE/>.

5 Experiments

Table 1 presents a comparative evaluation of KGCM-VAE against established causal time-series models using out-of-sample datasets. While baseline models such as Causal-TARNet and R-CRN exhibit slightly higher predictive precision—achieving the lowest Test RMSE at 0.2008 and 0.2034, respectively—they demonstrate limitations in causal discovery. Most notably, KGCM-VAE achieves the superior PEHE (3.8159), marking a significant improvement in treatment effect estimation over all competitors. This divergence suggests that while standard models are optimized for minimizing forecasting error (RMSE), they often fail to accurately capture the counterfactual dynamics necessary for reliable causal inference. The robust PEHE performance of KGCM-VAE underscores its advantage in disentangling temporal correlations from true causal structures, making it a more reliable tool for decision-support systems where effect estimation is the primary objective.

Table 2 presents an ablation study evaluating the relative contributions of the Maximum Mean Discrepancy (MMD) and Causal Adjacency (ADJ) components to the model’s performance in terms of Treatment Effect Estimation error

Table 1. Benchmarking KGCM-VAE at treatment lag = 1 against causal time-series models on out-of-sample (Testing) datasets. PEHE measures the error in causal response estimation.

Model	Test RMSE	Test PEHE
KGCM-VAE	0.3225	3.8159
R-CRN	0.2034	3.8567
CF-RNN	0.2280	3.8599
Causal-TARNet	0.2008	3.8920

(PEHE). The results demonstrate that the integrated configuration, incorporating both MMD and ADJ constraints, achieves the superior performance with the lowest PEHE of 3.7939. This finding underscores the importance of the synergy between distributional balancing and structural causal priors; specifically, the inclusion of both components appears to regularize the latent space more effectively than either component in isolation. When the MMD component is removed (3.8581) or the ADJ constraint is excluded (3.8760), the model exhibits an increase in estimation error, suggesting that neither auxiliary regulator is sufficient on its own to fully capture the underlying causal dynamics. Notably, the configuration excluding both components yields a PEHE of 3.8667, confirming that the proposed MMD and ADJ modules provide critical structural information that goes beyond the capabilities of the baseline VAE-GRU backbone. Overall, these results highlight that the joint application of these constraints is essential for achieving the most accurate and robust causal inference in time-series settings.

Table 2. Ablation study of the KGCM-VAE model at treatment lag = 1 evaluating the impact of MMD and causal adjacency (ADJ) components on PEHE.

Model	Evaluation Metric		
	MMD	ADJ	PEHE
✓	✓		3.7939
✗	✓		3.8581
✓	✗		3.8760
✗	✗		3.8667

Table 3. Ablations of KGCM-VAE Across Different Treatment Lags

KGCM-VAE		
Treatment lag	RMSE	PEHE
3 days	0.3194	3.8204
6 days	0.3185	3.8304
9 days	0.3206	3.8390

The performance of the KGCM-VAE across varying temporal scales is detailed in Table 3. The results indicate that predictive accuracy is sensitive to the treatment lag, with the RMSE starting at 0.5513 for a 3-day lag, peaking at 0.7236 at 6 days, and subsequently improving to 0.6250 as the lag extends to 9 days. This non-linear trend suggests that a 6-day interval may represent a period of peak volatility or complex interaction within the Arctic sea ice dynamics that the model must navigate. In contrast, the model’s ability to estimate heterogeneous treatment effects demonstrates remarkable stability across all tested intervals. The PEHE varies only marginally between 0.0480 and 0.0485, confirming that the KGCM-VAE maintains a robust and consistent causal inference capability regardless of the specific temporal displacement of the treatment.

5.1 Real-World Validation and Sensitivity

The causal relationships illustrated in Figure 2 show the time-series evolution of velocity and SSH perturbations. By independently perturbing ocean velocity and ssh, the KGCM-VAE framework demonstrates a sophisticated capture of geostrophic and dynamic feedbacks—specifically, how the model responds to perturbed velocity-based and SSH-based treatments.

As these velocity and SSH drivers are modulated, the corresponding counterfactual predictions of sea ice thickness are shown in the bottom panels. The influence of SSH on sea ice thickness reflects the model’s ability to confirm the well-defined connection between ssh and sea ice thickness found in the literature [28].

Ultimately, the divergence between velocity-driven (Figure 2, left panel) and SSH-driven counterfactual outcomes demonstrates that the KGCM-VAE avoids treating these variables as interchangeable features. Instead, the model extracts distinct causal signals from each, allowing it to isolate and predict the Arctic system’s specific response to individual changes within the oceanic environment. It is noteworthy that the velocity-driven treatment did not influence the sea ice thickness prediction.

This case study illustrates (Figure 2, right panel) how perturbations in SSH influence sea ice thickness by comparing factual and counterfactual scenarios. The results show that changes in SSH lead to measurable differences in the temporal evolution of sea ice thickness, demonstrating a clear causal response. A study by [28] indicated that the impact of SSH operates primarily through sea ice dynamics by modifying sea ice drift, ice–ocean stress, and the gradient force, rather than through thermodynamic processes. These findings highlight the critical yet subtle role of SSH gradient forces in shaping sea ice thickness, without which the resulting thickness changes would be substantially different. Overall, our results are consistent with these established physical mechanisms.

6 Conclusion and Future Work

Our proposed algorithm, the Knowledge-Guided Causal Model Variational Autoencoder (KGCM-VAE), offers a robust VAE-based framework that integrates

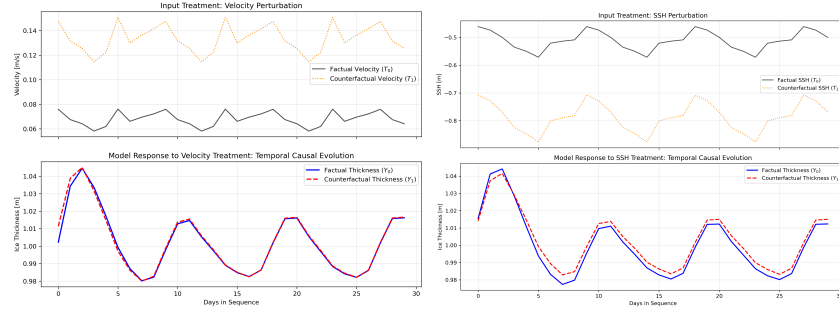


Fig. 2. Real-world spatial analyses of factual and counterfactual outcomes. The panels display the temporal patterns of perturbed Ocean Velocity (Top left) and the corresponding counterfactual prediction of Sea Ice Thickness (Bottom left), alongside perturbed Sea Surface Height (Top right) and the corresponding counterfactual prediction of Sea Ice Thickness (Bottom right).

domain knowledge for reliable causal inference in real-world spatiotemporal applications. By explicitly incorporating MMD within its architecture, KGCM-VAE effectively minimizes distributional discrepancies between treated and control covariate distributions in the learned latent space \mathbf{z} . In a real-world Arctic scenario, this balancing prevents the model from mistakenly attributing sea-ice thinning to ocean velocity changes when the true driver may be unobserved seasonal background warming. This crucial step ensures that the latent representations remain balanced and treatment-invariant. The unique combination of dynamic modeling and latent balancing enables the model to learn robust, disentangled representations that capture the underlying confounded system state. This disentanglement is further stabilized by the integration of causal modeling via an adjacency matrix within the decoder. Consequently, KGCM-VAE demonstrates superior performance in estimating the Precision in Estimation of Heterogeneous Effect (PEHE). Compared to established benchmarks, KGCM-VAE achieves a reduction in PEHE of approximately 1.06% over R-CRN and 1.95% over causal-TARNet. While the model's RMSE values were observed to be higher than those of baseline models, this highlights a deliberate and necessary trade-off: our method prioritizes causal accuracy and disentanglement over raw predictive fidelity. This focus is crucial for reliable counterfactual generalization beyond the observed training data. Furthermore, our ablation study underscores the critical role of latent space balancing; the inclusion of both MMD and Causal Adjacency (ADJ) components resulted in a 1.88% improvement in PEHE compared to the backbone model lacking these constraints. This confirms that these components are particularly useful for complex real-world datasets where accurate causal effect estimation within dynamic systems is required. Looking ahead, we plan to extend KGCM-VAE to further validate its generalizability and utility in addressing complex causal questions in high-dimensional spatial fields.

Acknowledgment This research is funded by the NSF grant from the HDR Institute: HARP - Harnessing Data and Model Revolution in the Polar Regions (2118285).

References

1. Runge, J., Gerhardus, A., Varando, G., Eyring, V. & Camps-Valls, G. Causal inference for time series. *Nature Reviews Earth & Environment*. **4**, 487-505 (2023).
2. Pearl, J. & Mackenzie, D. The book of why: the new science of cause and effect. (Basic books,2018)
3. Pearl, J. Causality. (Cambridge University Press, 2009).
4. Chapman, W., Welch, W., Bowman, K., Sacks, J. & Walsh, J. Arctic sea ice variability: Model sensitivities and a multidecadal simulation. *Journal of Geophysical Research: Oceans*. **99**, 919-935 (1994).
5. Walsh, J. & Johnson, C. Interannual atmospheric variability and associated fluctuations in Arctic sea ice extent. *Journal of Geophysical Research: Oceans*. **84**, 6915-6928 (1979).
6. Notz, D. & Marotzke, J. Observations reveal external driver for Arctic sea-ice retreat. *Geophysical Research Letters*. **39** (2012).
7. Reichstein, M., Camps-Valls, G., Stevens, B., Jung, M., Denzler, J., Carvalhais, N. & Prabhat, F. Deep learning and process understanding for data-driven Earth system science. *Nature*. **566**, 195-204 (2019).
8. Peters, J., Janzing, D. & Schölkopf, B. Elements of causal inference: foundations and learning algorithms. (The MIT Press, 2017).
9. Ahuja, K., Mahajan, D., Wang, Y. & Bengio, Y. Interventional causal representation learning. *International Conference on Machine Learning*. pp. 372-407 (2023).
10. Xu, H., Xu, Y., Li, C. & Zhuang, F. Causal structure representation learning of unobserved confounders in latent space for recommendation. *ACM Transactions on Information Systems*. (2025).
11. Gao, H., Li, J., Qiang, W., Si, L., Xu, B., Zheng, C. & Sun, F. Robust causal graph representation learning against confounding effects. *Proceedings of the AAAI Conference on Artificial Intelligence*. **37**, 7624-7632 (2023).
12. Runge, J., Nowack, P., Kretschmer, M., Flaxman, S. & Sejdinovic, D. Detecting and quantifying causal associations in large nonlinear time series datasets. *Science Advances*. **5**, eaau4996 (2019).
13. Wu, T., Wu, X., Wang, X., Liu, S. & Chen, H. Nonlinear causal discovery in time series. *Proceedings of the 31st ACM International Conference on Information & Knowledge Management*. pp. 4575-4579 (2022).
14. Schölkopf, B., Locatello, F., Bauer, S., Ke, N., Kalchbrenner, N., Goyal, A. & Bengio, Y. Toward causal representation learning. *Proceedings of the IEEE*. **109**, 612-634 (2021).
15. Austin, P. An introduction to propensity score methods for reducing the effects of confounding in observational studies. *Multivariate Behavioral Research*. **46**, 399-424 (2011).
16. Chipman, H., George, E. & McCulloch, R. BART: Bayesian additive regression trees. (2010).
17. Wager, S. & Athey, S. Estimation and inference of heterogeneous treatment effects using random forests. *Journal of the American Statistical Association*. **113**, 1228-1242 (2018).

18. Dudík, M., Langford, J. & Li, L. Doubly robust policy evaluation and learning. *ArXiv Preprint ArXiv:1103.4601*. (2011).
19. Athey, S. & Imbens, G. Recursive partitioning for heterogeneous causal effects. *Proceedings of the National Academy of Sciences*. **113**, 7353-7360 (2016).
20. Belloni, A., Chernozhukov, V. & Hansen, C. Inference on treatment effects after selection among high-dimensional controls. *Review of Economic Studies*. **81**, 608-650 (2014).
21. Shalit, U., Johansson, F. & Sontag, D. Estimating individual treatment effect: generalization bounds and algorithms. *International Conference on Machine Learning*. pp. 3076-3085 (2017).
22. Johansson, F., Shalit, U. & Sontag, D. Learning representations for counterfactual inference. *International Conference on Machine Learning*. pp. 3020-3029 (2016).
23. Yao, L., Li, S., Li, Y., Huai, M., Gao, J. & Zhang, A. Representation learning for treatment effect estimation from observational data. *Advances in Neural Information Processing Systems*. **31** (2018).
24. Tian, L., Alizadeh, A., Gentles, A. & Tibshirani, R. A simple method for estimating interactions between a treatment and a large number of covariates. *Journal of the American Statistical Association*. **109**, 1517-1532 (2014).
25. Berrevoets, J., Curth, A., Bica, I., McKinney, E. & Schaar, M. Disentangled counterfactual recurrent networks for treatment effect inference over time. *ArXiv Preprint ArXiv:2112.03811*. (2021)
26. Zhu, H., Huang, H., Yin, K., Fan, Z., Jin, H. & Liu, B. CausalNET: Unveiling causal structures on event sequences by topology-informed causal attention. *Proceedings Of The IJCAI*. pp. 7144-7152 (2024)
27. Shalit, U., Johansson, F. & Sontag, D. Estimating individual treatment effect: generalization bounds and algorithms. *International Conference On Machine Learning*. pp. 3076-3085 (2017)
28. Wang, Q., Danilov, S., Mu, L., Sidorenko, D. & Wekerle, C. Lasting impact of winds on Arctic sea ice through the ocean's memory. *The Cryosphere Discussions*. **2021** pp. 1-31 (2021)
29. Mo, Z., Liu, Q., Yan, B., Zhang, L. & Di, X. Causal adjacency learning for spatiotemporal prediction over graphs. *2024 IEEE 27th International Conference On Intelligent Transportation Systems (ITSC)*. pp. 621-626 (2024)
30. Ng, I., Zhu, S., Fang, Z., Li, H., Chen, Z. & Wang, J. Masked gradient-based causal structure learning. *Proceedings Of The 2022 SIAM International Conference On Data Mining (SDM)*. pp. 424-432 (2022)